J|A|C|S ARTICLES

Published on Web 10/26/2009

Breaking Mechanism of Single Molecular Junctions Formed by Octanedithiol Molecules and Au Electrodes

Yuanhua Qi,*,† Jingyu Qin,‡ Guoli Zhang,† and Tao Zhang†

School of Physics and School of Materials Science and Engineering, Shandong University, Jinan 250100, China

Received April 1, 2009; E-mail: yuanhuaqi@sdu.edu.cn

Abstract: We present a theoretical study of the elongation process of molecular junctions formed by octanedithiol molecule and Au electrodes. Five types of junctions that have different molecule−electrode coupling geometries are considered. It is found that the behavior of the H atom in the −SH group plays a crucial role in the system structure variation. The variation of the total energy and the average force needed to break the molecular junction are calculated, and each type of molecular junctions is found to have a characteristic breaking force. Comparing our theoretical results with those from experiment shows that the most probable coupling geometry was neglected in almost all the previous work. A dynamic analysis of the electronic structure of the molecular junctions is used to understand the variation of the system configuration.

1. Introduction

The potential use of a single molecule as an electronic device has attracted much attention in both experimental[1−8] and theoretical[9−13] studies. The molecular break junction (MBJ) approach[14−16] is often used to investigate the formation and breaking mechanism of molecular junctions. With this approach, molecular junctions formed via thiol (thiolate)−Au contacts have been studied extensively,[17−23] and many interesting results were obtained. However, unresolved questions still exist which are fundamental to the understanding of the MBJ experiment result. The first is regarding the nature of the bond between the −SH group and the Au electrode: is the end H atom detached in the formation of a junction? Some researchers believe it remains,[24,25] and some believe it is detached,[5,17,26−29] while some others believe that both cases may exist.[30−32] To the researchers who believe the H atom's being detached, the second question arises: according to the research work of Grönbeck,[30] the detached H

† School of Physics.
‡ School of Materials Science and Engineering.

(1) Chen, J.; Reed, M. A.; Rawlett, A. M.; Tour, J. M. *Science* **1999**, *286*, 1550–1552.
(2) Reed, M. A.; Chen, J.; Rawlett, A. M.; Price, D. W.; Tour, J. M. *Appl. Phys. Lett.* **2001**, *78*, 3735–3737.
(3) Bumm, L. A.; Arnold, J. J.; Cygan, M. T.; Dunbar, T. D.; Burgin, T. P.; Jones, L.; Allara, D. L.; Tour, J. M.; Weiss, P. S. *Science* **1996**, *271*, 1705–1707.
(4) Cui, X. D.; Primak, A.; Zarate, X.; Tomfohr, J.; Sankey, O. F.; Moore, A. L.; Moore, T. A.; Gust, D.; Harris, G.; Lindsay, S. M. *Science* **2001**, *294*, 571–574.
(5) Reed, M. A.; Zhou, C.; Muller, C. J.; Burgin, T. P.; Tour, J. M. *Science* **1997**, *278*, 252–254.
(6) Kergueris, C.; Bourgoin, J. P.; Palacin, S.; Esteve, D.; Urbina, C.; Magoga, M.; Joachim, C. *Phys. Rev. B* **1999**, *59*, 12505–12513.
(7) Liang, W.; Shores, M. P.; Bockrath, M.; Long, J. R.; Park, H. *Nature* **2002**, *417*, 725–729.
(8) Pobelov, I. V.; Li, Z.; Wandlowski, T. *J. Am. Chem. Soc.* **2008**, *130*, 16045–16054.
(9) Di Ventra, M.; Pantelides, S. T.; Lang, N. D. *Phys. Rev. Lett.* **2000**, *84*, 979–982.
(10) D'Agosta, R.; Di Ventra, M. *J. Phys.: Condens. Matter* **2008**, *20*, 374102(1−10).
(11) Taylor, J.; Brandbyge, M.; Stokbro, K. *Phys. Rev. Lett.* **2002**, *89*, 138301(1−4).
(12) Zoloff Michoff, M. E.; Vélez, P.; Leiva, E. P. M. *J. Phys. Chem. C* **2009**, *113*, 3850–3854.
(13) Kazunari, Y.; Tomofumi, T.; Aleksandar, S. *J. Am.Chem.Soc.* **2008**, *130*, 9406–9413.
(14) Park, H.; Park, J.; Lim, A. K. L.; Anderson, E. H.; Alivisatos, A. P.; McEuen, P. L. *Nature* **2000**, *407*, 57–60.
(15) Weber, H. B.; Reichert, J.; Weigend, F.; Ochs, R.; Beckmann, D.; Mayor, M.; Ahlrichs, R.; von Lohneysen, H. *Chem. Phys.* **2002**, *281*, 113–125.
(16) Smit, R. H. M.; Noat, Y.; Untiedt, C.; Lang, N. D.; van Hemert, M. C.; van Ruitenbeek, J. M. *Nature* **2002**, *419*, 906–909.
(17) Xu, B. Q.; Tao, N. J. *Science* **2003**, *301*, 1221–1223.
(18) Reddy, P.; Jang, S. Y.; Segalman, R. A.; Majumdar, A. *Science* **2007**, *315*, 1568–1571.
(19) Tsutsui, M.; Taniguchi, M.; Kawai, T. *Nano Lett.* **2008**, *8*, 3293–3297.
(20) Salomon, A.; Cahen, D.; Lindsay, S.; Tomfohr, J.; Engelkes, V. B.; Frisbie, C. D. *Adv. Mater.* **2003**, *15*, 1881–1890.
(21) Park, J.; Pasupathy, A. N.; Goldsmith, J. I.; Chang, C.; Yaish, Y.; Petta, J. R.; Rinkowski, M.; Sethna, J. P.; Abruña, H. D.; McEuen, P. L.; Ralph, D. C. *Nature* **2002**, *417*, 722–725.
(22) Reichert, J.; Ochs, R.; Beckmann, D.; Weber, H. B.; Mayor, M.; von Löhneysen, H. *Phys. Rev. Lett.* **2002**, *88*, 176804.
(23) Akkerman, H. B.; Blom, P. W. M.; de Leeuw, D. M.; de Boer, B. *Nature* **2006**, *441*, 69–72.
(24) Rzeünicka, I. I.; Lee, J.; Maksymovych, P.; Yates, J. T. *J. Phys. Chem. B* **2005**, *109*, 15992–15996.
(25) Maksymovych, P.; Sorescu, D. C.; Yates, J. T. J. *J. Phys. Chem. B* **2006**, *110*, 21161–21167. Maksymovych, P.; Sorescu, D. C.; Dougherty, D.; Yates, J. T. *J. Phys. Chem. B* **2005**, *109*, 22463–22468. Maksymovych, P.; Yates, J. T. J. *J. Am. Chem. Soc.* **2008**, *130*, 7518–7519.
(26) Kodama, C.; Hayashi, T.; Nozoye, H. *Appl. Surf. Sci.* **2001**, *169*−*170*, 264–267.
(27) Liu, G.; Rodriguez, J. A.; Dvorak, J.; Hrbek, J.; Jirsak, T. *Surf. Sci.* **2002**, *505*, 295–307.
(28) Laibinis, P. E.; Whitesudes, G. M.; Allara, D. L.; Tao, Y.; Parikh, A. N.; Nuzzo, R. G. *J. Am. Chem. Soc.* **1991**, *113*, 7152–7162.
(29) Xu, B. Q.; Xiao, X. Y.; Tao, N. J. *J. Am. Chem. Soc.* **2003**, *125*, 16164–16165.
(30) Grönbeck, H.; Curioni, A.; Andreoni, W. *J. Am. Chem. Soc.* **2000**, *122*, 3839–3842.
(31) Nuzzo, R. G.; Zegarski, B. R.; Dubois, L. H. *J. Am. Chem. Soc.* **1987**, *109*, 733–740.
(32) Zhou, J. G.; Hagelberg, F. *Phys. Rev. Lett.* **2006**, *97*, 045505(1−4) .

10.1021/ja902573e CCC: $40.75

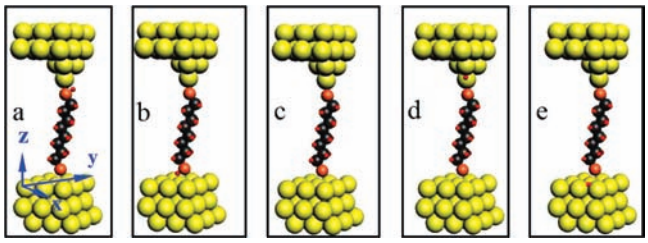

Figure 1. Five types of molecular junctions considered in our simulation. In (a) and (b), the end H atom of the junction at the tip (T1) or substrate (T2) side is retained; in (c) no end H atom is retained (T3). In (d) and (e), one detached H atom is adsorbed to the Au tip (T4) and substrate (T5), respectively. In (a) we show the reference frame of our calculation.

atoms are adsorbed by the Au surface, and then do these H atoms have any influence on the mechanical and transport properties of the junction? This question has been neglected by almost all researchers. The third is about the break geometry of the molecular junction: where does the breakdown take place? Is it in the S−Au, Au−Au, or S−C bond? The answer to the last question may be highly relevant to that of the second one. It is difficult to show directly the detailed coupling geometry in the MBJ experiment, and therefore a systematic theoretical study of the MBJ process is necessary.

We present here a theoretical study of the MBJ processes of molecular junctions formed by octanedithiol molecules and Au electrodes. The contraction and elongation processes are simulated, and the variation of the total energy and the average force to break the molecular junction are calculated. A dynamic analysis of the electronic structure is used to understand the structure variation of the junction. Compared with the theoretical method most frequently used in probing the bond nature of a junction, which is based on comparison of the adsorption energies,[30,32] the advantage of this method is that the result can be directly compared with that of the MBJ experiment and therefore provides straightforward support to the experiment.

2. Computational Methods and Simulation Protocol

In the MBJ experiment, which uses scanning tunneling microscopy (STM), the STM tip is first brought into contact with the molecule adsorbed to the substrate to form the molecular junction and then drawn back gradually until the breakdown takes place. A simple and valid model of the tip, the substrate, and the coupling geometries in the molecule−substrate and molecule−tip contacts is crucial to a simulation. In this work, we use three layers (3×3) of Au atoms with face-centered-cubic crystal structure of the (111) surface to model the substrate, two layers of Au atoms with same structure as in the substrate, and a four-atom pyramid structure to represent the tip. Repeating periodically, the atom layers in the substrate and tip form infinite surfaces, while in the direction perpendicular to the surface, they join perfectly to form five layers of Au surface. Five types of initial coupling geometries between the molecule and the electrodes are taken into consideration, as we show in Figure 1, and we will refer to them as T1, T2, T3, T4, and T5 in the following text. In T1, the end H atom at the substrate side is detached, while that at the tip side remains. In T2, the situation is just the opposite. In T3, both end H atoms are detached. T4 and T5 are similar to T3, but one detached H atom is adsorbed to the tip or substrate Au atom to which the molecule is attached. In the initial junction geometries of the simulation, the structures of the substrate, the tip, and the molecule are set as they are in the independently relaxed system, and the Au−S bond lengths on both sides are set to the optimized value. T1, T2, and T3 are the most preferable molecular junctions according to the recent studies.[24−32] T4 and T5 come from our study on the dissociation process of molecules with the −SH group on the Au substrate and tip. It is found that, as the end H atom is detached, it first occupies a site around the Au atom to which the molecule is adsorbed. On the substrate, it is a hollow site, and the equilibrium distances from the H atom to the three Au atoms are 1.95, 1.91, and 1.81 Å, respectively, while on the tip, it is a bridge site between the topmost atom and a base atom of the pyramid structure, with the equilibrium distances to the two Au atoms being 1.82 and 1.73 Å, respectively. In the initial structure of T4 and T5, we set the position of the detached H atom according to these values. These two types of junctions are introduced to check the effect of the detached H atom on the mechanical properties of the molecular junction.

To include as many different coupling geometries between the molecule and electrodes as possible in our simulation, besides the above considerations, in each type of molecular junction, T1−T5, different sites for adsorption of the molecule to the substrate surface and the azimuthal angle of the molecule (the angle of the plane containing all the C atoms of the molecule with respect to the x axis) in the initial configuration are tested. Some geometrical parameters, the adsorption energies of the molecule to the two electrodes in the five types of junctions, and a comparison with other theoretical work are shown in the Supporting Information.

In the current simulation we adopt a protocol that is similar to but improved over the one we used in the previous works.[33,34] In order to make good contact of the molecule with the tip and the substrate, starting from the initial structure shown by Figure 1, we contract the junction by about 1−2.0 Å first. After the contraction, we elongate it gradually until the breakdown takes place. The elongation (contraction) process is performed in a sequence which consists of many similar steps. In each step, the tip Au atoms are first moved apart from (toward) the substrate by 0.2 Å; in the mean time, the lattice parameter in the stretch direction of the molecular junction is increased (decreased) by 0.2 Å; and then, with the z coordinates of the Au atoms in the two end layers of the junction fixed, the x and y coordinates of these atoms and all the coordinates of the other atoms in the junction are relaxed until the force on each of them is less than 0.08 nN (0.05 eV/Å). The atomic structure at the end of the current step is set as the beginning of the next one, and this process continues until the breakdown takes place (or the system is contracted by 1−2 Å). With the above protocol, we in fact simulate the adiabatic stretching process[35,36] that occurs at a high stretching rate.

All the calculations in this paper are based on *ab initio* total energy density functional theory (DFT)[37,38] and conducted with the SIESTA code.[39] The PEB-GGA[40] and norm-conserving pseudopotentials[41] are used. The wave functions are expanded in a numerical basis set.[42] The single-ζ basis with a polarization function is used for Au atoms and double-ζ basis with a polarization function for the other atoms. The 2×2×2 Monkhorst-Pack k point sampling is used in all the simulations. To verify the validity of the current methods, we calculate the lattice constant of the bulk Au and the S−C and S−H bond lengths in the isolated CH_3SH molecule. The corresponding values are 4.20, 1.83, and 1.38 Å, respectively, which

(33) Qi, Y.; Guan, D.; Jiang, Y.; Liu, C.; Zhang, D. *Appl. Phys. Lett.* **2006**, *89*, 182119–182121.
(34) Qi, Y.; Guan, D.; Jiang, Y.; Zheng, Y.; Liu, C. *Phys. Rev. Lett.* **2006**, *97*, 256101(1−4).
(35) Huang, Z.; Chen, F.; Benett, P. A.; Tao, N. J. *J. Am. Chem. Soc.* **2007**, *129*, 13225–13231.
(36) Li, X. L.; He, J.; Hihath, J.; Xu, B. Q.; Lindsay, S. M.; Tao, N. J. J. *Am.Chem. Soc.* **2006**, *128*, 2135–2141.
(37) Hohenberg, P.; Kohn, W. *Phys. Rev.* **1964**, *136*, B864–B871.
(38) Kohn, W.; Sham, L. J. *Phys. Rev.* **1965**, *140*, A1133–A1138.
(39) Soler, J.; Artacho, E.; Gale, J.; García, A.; Junquera, J.; Ordejón, P.; Sánchez-Portal, D. *J. Phys.: Condens. Matter* **2002**, *14*, 2745–2779.
(40) Perdew, J. P.; Burke, K.; Ernzerhof, M. *Phys. Rev. Lett.* **1996**, *77*, 3865–3868.
(41) Troullier, N.; Martins, J. L. *Phys. Rev. B* **1991**, *43*, 1993–2006.
(42) Artacho, A.; Sánchez-Portal, D.; Ordejón, P.; Garcia, A.; Soler, J. M. *Phys. Status Solidi B* **1999**, *215*, 809–817.

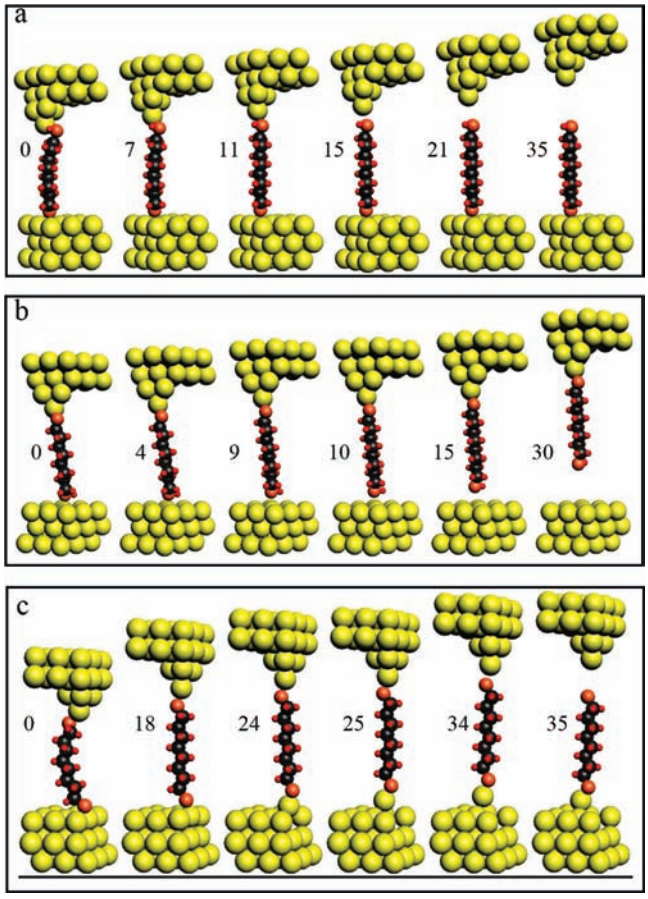

Figure 2. Structure evolution of junctions (a) T1, (b) T2, and (c) T3. The numbers denote the elongation step. At step 0 (initial step of the elongation), the lengths of these three junctions are 28.3, 29.1, and 28.3 Å, respectively.

are consistent with the experimental values (4.08, 1.82, and 1.34 Å).[43] We also calculate the cohesive energy of the bulk Au and get a value of 4.11 eV, which is also in good agreement with the experimental value (3.81 eV).[43]

3. Results and Discussion

3.1. Structure Evolution. With the above protocol, we simulate the contraction and elongation processes of the five types of molecular junctions. Our simulation clearly shows that each type of molecular junction has a characteristic elongation process in which the main feature of the structural variation is almost independent of the adsorption sites and azimuth of the molecule in the initial step. The molecule will become bent during contraction and straight during elongation, but the changes of the C−C and C−H bond lengths are smaller than 1.5% (see movies in the Supporting Information for a more intuitive understanding).

Figure 2a,b shows the structure evolution of T1 and T2 during the elongation. No visible structure variation is found in the substrate and tip, and both junctions break at the thiol−Au bond

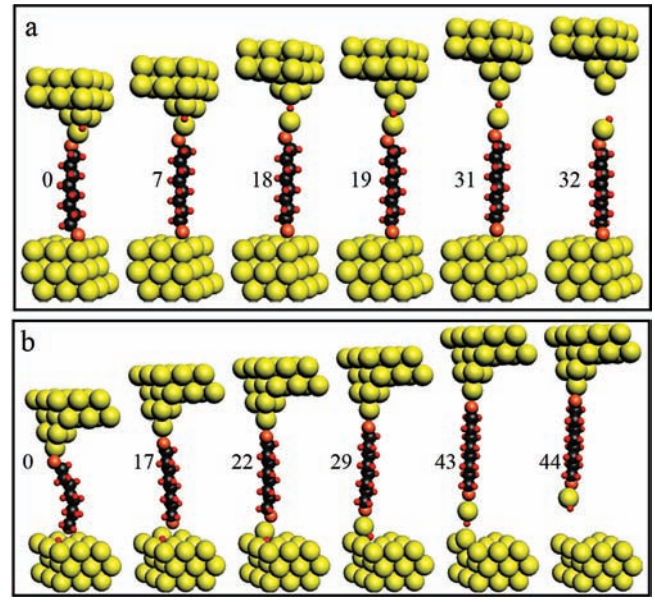

Figure 3. Structure evolution of junctions (a) T4 and (b) T5. The numbers denote the elongation step. The lengths of these two junctions at step 0 (initial step of the elongation) are 29.7 and 28.3 Å, respectively.

at last. This indicates that the thiol−Au bond is weaker than the thiolate−Au bond.

Figure 2c shows the structure evolution of T3. During the elongation, the evident change in the substrate is that a Au atom is pulled out from the surface, but instead of breaking between this Au atom and the substrate, the junction at last breaks at the S−Au bond on the tip side.

Figure 3 shows the structure evolution of T4 and T5. For these two types of junctions, the rupture always takes place at the side with the H atom adsorbed. During the elongation, the H atom gradually enters into the interval between two Au atoms in the tip or substrate. This makes the breakdown take place at the Au−H bond at last. This breaking mechanism has never been mentioned before, and we will show in the later text that it may be the most important mechanism in the MBJ experiment involving a SH−Au contact.

The effect of the adsorption site of the detached H atom on the breaking geometry of T4 has been considered in our simulation, and it is found that if this H atom is adsorbed to a site around which no octanedithiol molecule is attached, the junction is broken at the Au−S bond at last, just as in T3. That is to say, only when the H atom is absorbed to the site near the Au atom to which the molecule is attached can it have effects on the breaking geometry of the molecular junction (see movies in the Supporting Information for details).

To reach a more general conclusion, we need to consider a different type of tip structure in which there exists a short single Au chain. In this case, the junction may have a different breaking geometry. However, considering that the break junction experiments are often done at ambient temperature, we perform a dynamic simulation of the equilibration process of the isolated electrode at 300 K and find that the pyramid structure at the tip is very stable, while the short chain structure is destroyed rapidly. Therefore, we deduce that the short chain structure cannot possibly exist in the initial electrodes in a MBJ experiment (see Supporting Information for details).

In total, three different types of breaking geometries are found in our simulation: the junction can break at the thiol−Au,

(43) Kordis, J.; Gingerich, K. A.; Seyse, R. J. *J. Chem. Phys.* **1974**, *61*, 5114–5121. Huber, K. P; Herzberg, G. *Molecular Spectra and Molecular Structure: Constants of Diatomic Molecules*; Van Nostrand Reinhold: New York, 1979; Vol. IV. Harmony, M. D.; Laurie, V. W.; Kuczkowski, R. L.; Schwendeman, R. H.; Ramsay, D. A.; Lovas, F. L.; Lafferty, W. J.; Maki, A. G. *J. Phys. Chem. Ref. Data* **1979**, *8*, 619–721. Khein, A.; Singh, D. J.; Umrigar, C. J. *Phys. Rev. B* **1995**, *51*, 4105V.

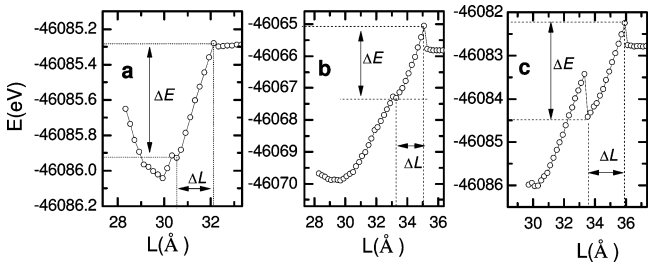

Figure 4. Three typical total energy−junction length curves corresponding to (a) T1, (b) T3, and (c) T4.

Table 1. Breaking Bond Type and Breaking Force of the Five Types of Molecular Junctions[a]

	junction type				
	T1	T2	T3	T4	T5
breaking bond	thiol−Au	thiol−Au	S−Au	H−Au	H−Au
breaking force	0.6 ± 0.2	0.6 ± 0.2	2.2 ± 0.2	1.5 ± 0.2	1.5 ± 0.2

[a] The breaking bond refers to the bond break at the last stage of the elongation. The force is in nN.

thiolate−Au, and H−Au bonds, respectively. The junction always breaks at the thiol−Au bond if one exists. Adsorption of the detached H atom to the electrode Au atom around the molecule significantly changes the structure evolution of the junction.

3.2. Energy Variation and Breaking Force. To gain insight into the structure evolution of molecular junctions during the elongation, we calculate the variation of the total energy with the junction length L of the five types of junctions. Here the junction length L is defined as the size of the supercell in the stretch direction (the z axis). The result shows that each of the total energy−junction length curves can be divided into several well-defined segments which are usually separated by abrupt changes in energy. The tendency of the energy variation is roughly the same in each segment but different between two neighboring ones. Figure 4 shows the three typical energy−junction length curves corresponding to T1, T3, and T4. Inspecting the coordinates of the junction atoms in each step shows that the system structure varies gradually in the same segment but undergoes an abrupt change from one segment to another. The last segment describes the energy variation after the breakdown of the junction, and the energy keeps a roughly constant value. We define the segment before the last one as the breaking segment and the corresponding process as the breaking process. The molecular junction breaks during this process. We define the average force during the breaking process as breaking force (F); therefore, the breaking force can be written as

$$F = \Delta E/\Delta L$$

where ΔE and ΔL are the changes of the total energy and length of the molecular junction in the breaking process, respectively. In Table 1 we list the calculated breaking force of the five types of molecular junctions shown in Figure 1. For comparison, we also simulate the breaking process of a four-atom single Au chain and get a breaking force of 1.6 nN. This value is consistent with the one measured by Rubio et al.[44]

As we can see from Table 1, the value of the breaking force of a molecular junction is mainly determined by the type of the breaking bond at the last stage of the elongation. Each of these bonds has a characteristic breaking force. The thiol−Au bond has the smallest breaking force, and the S−Au bond has the biggest one. T1 and T2 have equal breaking forces and may be undistinguishable in the experiment; the same is true for T4 and T5.

The MBJ process of the octandithiol−Au junction has been experimentally studied by Li et al.,[36] and the average breaking force was determined to be ∼1.6 nN. According to this result, the authors concluded that the molecular junction is broken at the Au−Au bond, because the Au−Au bond has a well-known breaking force value ∼1.6 nN. However, as shown by our simulation, the breaking force of the H−Au bond is very close to that of the Au−Au bond. This suggests that T4 and T5 may be important molecular junctions in the experiment. That is to say, the adsorption of the detached H atom to the electrode plays a crucial role in the structure evolution of a molecular junction during elongation.

Another evidence for the conclusion that T4 and T5 may be important molecular junctions in the experiment comes from our study of the interaction between the molecule and tip. In this study we consider three different structures: the nondissociative molecule being adsorbed to the pure Au tip, the dissociative molecule being adsorbed to the pure Au tip, and the dissociative molecule being adsorbed to the Au tip with an H atom adsorbed. The result shows that the total energy of the third structure is almost equal to (slightly lower than, in fact) that of the first one, and the adsorption energy of the molecule in the third structure is the biggest. All the above observations suggest a possible transfer from the first structure to the third one and the formation of junctions T4 and T5 in the experiment (see Supporting Information for details).

According to the analysis above, we may conclude that the H atoms at both ends of the octanedithiol molecule are detached during the formation of a junction. The detached H atoms are adsorbed to the Au electrode. What the experiment measured are junction with S−Au bonds at both sides and H atoms adsorbed to the Au substrate and tip. During elongation, the junction breaks at the H−Au bond.

3.3. Dynamic Electronic Structure Analysis. With the molecular junction structures we get in the simulation, the electronic structures of the junctions at each elongation step are calculated, and a dynamic analysis of the density of states (DOS) can be performed. We will show below that the dynamic DOS analysis provides a good way to understand the structure variation during the deformation of the molecular junction. For the convenience of analysis, the projected DOS (PDOS) on a specific atom is calculated. The reference frame in our analysis is shown in Figure 1a.

Figure 5a shows the variation of the total PDOS on the S atom at the break point of T3. In Figure 5b we decompose the total PDOS to the s and p orbitals. No sp hybridization is found in this S atom. The sharp peak in the total DOS around the Fermi level can be attributed to the lone pair states of the p orbitals. It is mainly from the p_y orbital, and no variations in both shape and position are evident during the elongation. The peak in the p_z DOS around −5 eV (peak 1) shows only a subtle change during the breaking process, while the p_x DOS changes markedly. Inspecting the structure variation reveals that the change in the length of the S−C bond (0.03 Å) is much smaller than that of the S−Au bond (0.3 Å). We therefore attribute peak 1 of the p_z DOS to the S−C bond and that of the p_x DOS to the S−Au bond. Because peak 1 is in a low energy position relative

(44) Rubio, G.; Agraıt, N.; Vieira, S. *Phys. Rev. Lett.* **1996**, *76*, 2302–2035.

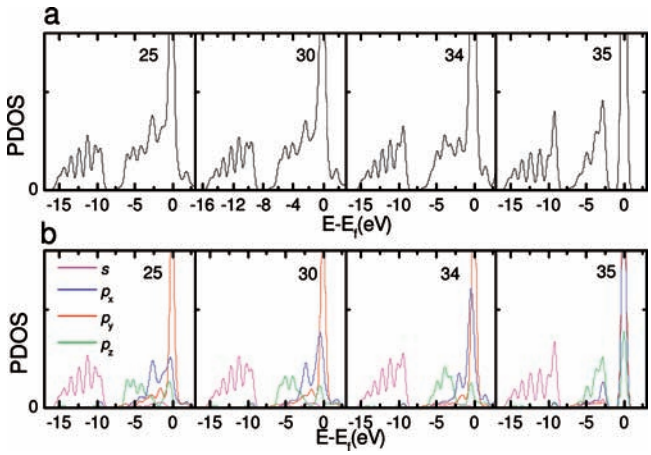

Figure 5. Variation of the PDOS on the S atom at the break point of T3. The number in each panel denotes the elongation step. Note that the junction breaks at step 35; steps 25, 30, and 34 are in the breaking process.

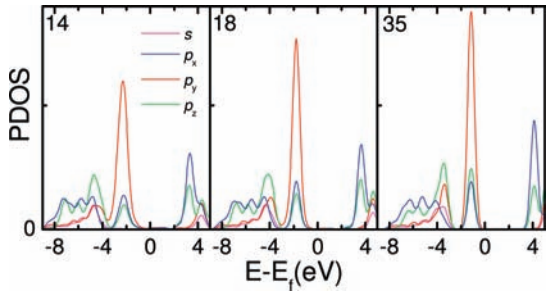

Figure 6. Variation of the PDOS on the S atom at the break point of T1. The number in each panel denotes the elongation step. Note that the junction breaks at step 20; steps 14 and 18 are in the breaking process. Step 35 is after the breakdown of T1.

to the p_x DOS, the S−C bond is stronger than the S−Au bond, and therefore T3 breaks at the S−Au bond instead of the S−C bond.

Figure 6 shows the variation of the PDOS on the S atom around the break point of T1. All peaks in the PDOS curves show a total shift to the high energy direction, and no visible changes in both shape and relative position are found during the elongation. This indicates the physical adsorption nature of the −SH group to the Au electrode and explains why the breaking force of the thiol−Au bond is the smallest. The hybridization between the s and p orbitals of the S atom can be clearly seen from Figure 6, which suggests very different electronic structures betweenT3 and T1.

Figure 7 shows the variation of the PDOS on the Au atom at the break point of T4. It is found that the $d_{x^2-y^2}$ and d_{xy} DOS are mainly from the lone pair electron in the d orbital and almost invariable in the breaking process; therefore, only the d_{yz}, d_{z^2}, d_{xz}, and s DOS are shown. The d_{yz}, d_{z^2}, and s DOS change very little during the breaking process. Checking the structure variation shows that the relative positions of the three Au atoms on the top of the adsorbed H atom are almost invariable during the breaking process, and hence we attribute the d_{yz}, d_{z^2}, and s DOS to the bonds between this Au atom and the two top Au atoms. The variation of the d_{xz} DOS shows the feature of the bond break,[34] and undoubtedly it is from the Au−H bond. The energy difference between the bonding and antibonding states (1.2 eV) at step 24 reflects the strength of the H−Au interaction.

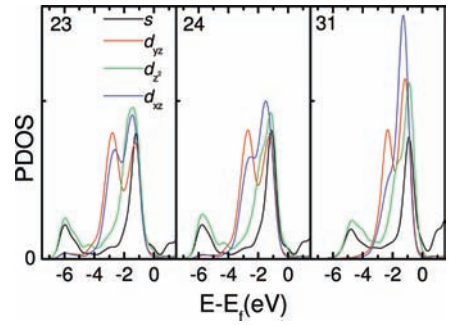

Figure 7. Variation of the PDOS on the Au atom at the break point of T4. The number in each panel denotes the elongation step. Note that steps 23, 24, and 31 are in the breaking process.

4. Conclusion

We have presented a theoretical study of the MBJ processes of the molecular junctions formed by octanedithiol molecules and Au electrodes. The five types of junctions most likely to exist are considered, and it is found that each of them has a characteristic breaking geometry and breaking force. The behavior of the end H atom in the −SH group plays a crucial role in the variation of the junction structure. As a detached H atom is adsorbed to the electrodes, it may enter into the interval between two Au atoms during the elongation, which causes the junction to break at the H−Au bond. By comparing our theoretical result with that of the experiment, it is found that the breakdown of the H−Au bond may be the most important mechanism in the MBJ experiment if the molecular junction contains SH−Au contacts. The breaking mechanism of the molecular junctions is understood from the dynamics analysis of the electronic structure.

Acknowledgment. This work was supported by the Natural Science Foundation of China (NSFC) (Grant Nos.10774089, 50671054) and Natural Science Foundation of Shandong Province (Grant Nos. Y2007A19).

Supporting Information Available: Structure and stability information about the molecular junctions studied. This material is available free of charge via the Internet at http://pubs.acs.org.

JA902573E